


Cite this: *New J. Chem.*, 2017, 41, 6385

# Water-soluble lanthanide complexes with a helical ligand modified for strong luminescence in a wide pH region†

 Shuhei Ogata,<sup>a</sup> Tomohito Shimizu,<sup>a</sup> Takashi Ishibashi,<sup>a</sup> Yushi Ishiyone,<sup>a</sup> Mitsuhiro Hanami,<sup>a</sup> Minami Ito,<sup>a</sup> Ayumi Ishii,<sup>a</sup> Shogo Kawaguchi,<sup>b</sup> Kunihsa Sugimoto<sup>b</sup> and Miki Hasegawa \*<sup>a</sup>

The luminescence and structure of a water-soluble helicate Eu complex with L<sup>COOH</sup>, which is a hexadentate ligand with COOH groups, were examined in solutions of various pH. The Eu complex EuL<sup>COOH</sup> is more than eight-coordinated around Eu, and one of the two carboxylate groups is not bound, even in the powdered state, based on the FT-IR measurement. The synchrotron X-ray powder diffraction peaks of EuL<sup>COOH</sup> broadened because of amorphous-like aggregation. EuL<sup>COOH</sup> retains the ff emission of Eu in a wide pH range of 2.6–9.7 and shows spectral reversibility at pH = 1.9–11.9. From Horrocks' equation, the number of coordinated water molecules to Eu of EuL<sup>COOH</sup> in the initial condition ( $3.0 \times 10^{-5}$  mol cm<sup>-3</sup>; pH 2.6–9.7) was estimated to be 1, but it increased in both strongly alkaline and acidic solutions. Molecular structural changes in these solutions were assumed from the quantum yields and electrospray ionization-mass spectrometry measurements. For instance, one carboxyl group of EuL<sup>COOH</sup> could provide hydrophilicity in the initial condition, and the other would be released from Eu at pH 2.1–2.6. Furthermore, EuL<sup>COOH</sup> decomposes below pH 1.9, but recovers with adjustments toward the initial pH. The ff emission of TbL<sup>COOH</sup> with a coordinated water molecule also appears in the green wavelength region in the initial condition. The luminescence ability of TbL<sup>COOH</sup> in water is higher than that in its powder. The luminescence processes of these complexes are discussed as an energy relaxation through the excited triplet state of L<sup>COOH</sup> assigned from the phosphorescence band of GdL<sup>COOH</sup>.

Received 29th April 2017,  
Accepted 1st June 2017

DOI: 10.1039/c7nj01444a

rsc.li/njc

## 1. Introduction

Water-soluble lanthanide complexes with strong luminescence are fascinating and can be applied to biological responses,<sup>1–13</sup> such as bio-probing, bio-imaging,<sup>14–34</sup> and *in situ* sensing of chemical species for pH, p<sup>1</sup>O<sub>2</sub>,<sup>35–42</sup> and metal ions.<sup>43–45</sup> The electronic absorption coefficient is quite low because the ff transitions of the lanthanide ion are Laporte forbidden, and it is difficult to obtain a strong ff emission by direct excitation. Thus, aromatic ligand moieties act to sensitize lanthanide luminescence as an antenna effect.<sup>46–48</sup> Luminescence of lanthanide complexes takes advantage of the narrow emission

band width (<10 nm full width at half maximum), long excited state lifetimes, and large Stokes shifts (>150 nm), which easily distinguish these complexes from excitation light and the shorter-lived background in biological systems.<sup>1,5</sup> Developing sufficiently bright and stable lanthanide complexes in aqueous solutions is a challenging research topic.<sup>49–61</sup>

The first visualization of living cells by lanthanide complexes was reported by Scaff *et al.* in 1969.<sup>14</sup> They used a luminescent Eu complex with 4,4,4-trifluoro-1-(2-thienyl)-1,3-butanedione to lyse a microorganism (*Bacillus megaterium*) and successfully observed luminescence of the whole cell using luminescence microscopy. Soini *et al.* developed an Eu luminescence label with the ligand of an ethylenediaminetetraacetic acid (EDTA) derivative localized on rabbit immunoglobulin G for time-resolved fluorescence microscopic observations.<sup>15</sup> There are many recent papers related to luminescent lanthanide complexes for the microscopic observation of biological science. Water-soluble Eu and Tb complexes with triethylenetetramine hexaacetic acid, a derivative of EDTA, migrated into the cytoplasm of adherent HeLa cells for imaging using a time-gated methodology.<sup>29</sup> These complexes, which are bridged by

<sup>a</sup> College of Science and Engineering, Aoyama Gakuin University, 5-10-1 Fuchinobe, Chuo-ku, Sagami-hara, Kanagawa, 252-5258, Japan.

E-mail: hasemiki@chem.aoyama.ac.jp; Fax: +81-42-759-6221

<sup>b</sup> Research & Utilization Division, Japan Synchrotron Radiation Research Institute (JASRI/SPring-8), 1-1-1 Kouto, Sayo, Hyogo 679-5198, Japan

† Electronic supplementary information (ESI) available: Attenuated total reflection FT-IR, electronic absorption, excitation and luminescence spectra with their decay profiles. For the syntheses, reaction scheme, ESI-MS and <sup>1</sup>H-NMR spectra, see DOI: 10.1039/c7nj01444a



cyclohexyldiamine, show intracellular stability, diffuse freely throughout the cytoplasm and nucleus, and do not partition to particular organelles.

1,4,7,10-Tetraazacyclododecane, a so-called cyclen, is known as one of the most stable ligand coordinating lanthanide ions, and there are hundreds of reports related to their luminescence properties, even in aqueous solutions.<sup>13,40</sup> Parker *et al.* reported various kinds of cyclen derivatives with lanthanide ions for bio-molecular sensing.<sup>11,30,34</sup> A cationic cyclen-based Eu complex exhibiting two-photon absorption (2PA) was recently reported for bio-imaging of living cells using near-infrared excitation.<sup>26</sup> Based on spectral analysis and the optimized molecular structure, the complex likely provides hydrophilicity in a cell; this was revealed by the observation of 2PA microscopy imaging on living T24 human cancer cells.

The proton concentration also becomes a key to determining the atmosphere in and around the bio-molecules.<sup>4</sup> Eu complexes with carboxyl-functionalized 1,5-naphthylridine derivatives demonstrate a pH-sensitive luminescence intensity from the isomerization of the ligand between keto-amine and enol-imine.<sup>37</sup> The Eu complex with the enol-imine ligand in a high pH solution luminesces stronger than that at a lower pH. The isomerization effect causes absorption band shifts of the ligand and suppresses the deactivation process from the solvent interaction.

2,2',6'2''-Terpyridine (terpyridine) is one of the most promising alternatives for absorbing and transferring the excitation energy to the lanthanide ion.<sup>61–65</sup> The derivatives of lanthanide complexes with a terpyridine skeleton have also been examined from the view point of analytical chemistry.<sup>66–71</sup> Eu and Tb complexes with terpyridine polyacidic derivatives were reported as luminescence sensors for time-resolved luminescence detection of the pH value in HeLa cells.<sup>67</sup> The luminescence of this Eu complex depends on the pH values, and the mixing solution of Eu and Tb complexes detects the pH based on the intensity ratio of the Eu and Tb emissions.

Various self-assembled lanthanide helicates were summarized by Piguet and Bünzli for their fundamental applications, such as syntheses, crystallography, luminescence properties with circularly polarized phenomena, and biological probes.<sup>72</sup> Recently, we reported mono-nuclear helicate complexes with a series of lanthanide ions, LnL (Ln = Nd, Eu, Gd, Tb, Dy, and Ho).<sup>73,74</sup> The hexadentate ligand, L, consisted of two bipyridine moieties and ethylenediamine. From the single crystal X-ray structural analyses, all LnL molecules were isostructural. The strong luminescence of EuL appeared at 580, 595, 615, 650, and 685 nm by ultraviolet (UV) excitation in the solid state. The luminescence and structural behaviour of EuL were maintained, even in acetonitrile, because of the high solubility and chelating effect. The aim of the present investigation was the development of a water-soluble Eu complex for molecular/ion sensing using the advantage of luminescent EuL.

Our molecular design strategy is shown in Fig. 1. EuL decomposes in aqueous solutions but can be used to derive substitution on nitrogen atoms of the reduced azomethine moieties.<sup>75</sup> Here, two carboxyl groups were selected as hydrophilic skeletons

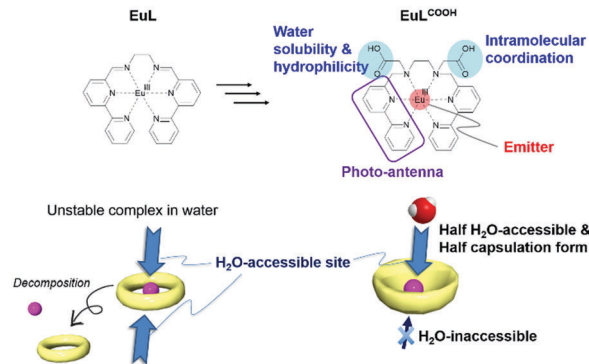


Fig. 1 Strategy of molecular design of this study.

and introduced into EuL, and the derivative is abbreviated as EuL<sup>COOH</sup>. Simultaneously, one of the carboxyl groups provides intramolecular coordination to Eu and the other provides solubility in water. The ligand forms a bowl shape, and the accessible area on Eu is an acting site for intermolecular interactions. Here, the luminescence properties of EuL<sup>COOH</sup> and TbL<sup>COOH</sup> are examined from the measurements of electronic absorption, luminescence, quantum yields, and lifetimes in the solid state and in water. GdL<sup>COOH</sup> was also prepared to determine the single and triplet states of the ligand. Electrospray ionization-mass spectrometry (ESI-MS) in various aqueous solutions, and attenuated total reflection Fourier transform infrared spectroscopy (ATR FT-IR), X-ray photoelectron spectroscopy (XPS), and synchrotron X-ray diffraction (XRD) in the solid state were performed to evaluate the structure. The dependence of the pH on the luminescence of EuL<sup>COOH</sup> is also discussed.

## 2. Results and discussion

### 2.1 Structure and luminescence of LnL<sup>COOH</sup> in the solid state

The L<sup>COOH</sup> ligand was newly synthesized through the reaction in Scheme S1 (ESI<sup>†</sup>) based on a literature procedure.<sup>76</sup> Reactions between L<sup>COOH</sup> and nitrates of Eu<sup>III</sup>, Gd<sup>III</sup>, and Tb<sup>III</sup> in ethanol formed the LnL<sup>COOH</sup> complexes. The detailed characterization is described in the experimental section.

An ATR FT-IR measurement was performed to assign the role of the two carboxylic acid groups in EuL<sup>COOH</sup>, and it was not necessary to consider counter anion exchange (Fig. 2). The O–H bending mode of the carboxyl group appears at 995 cm<sup>-1</sup> in L<sup>COOH</sup>. The 1730 and 1240–1203 cm<sup>-1</sup> bands in L<sup>COOH</sup> are assigned to the C=O and C–O stretching vibrations, respectively. After complexation with Eu, the corresponding O–H bending mode in the ligand remains at 946 cm<sup>-1</sup>. Similarly, the C=O stretching vibration mode in EuL<sup>COOH</sup> shifts to a lower energy (~1600 cm<sup>-1</sup>) than that for L<sup>COOH</sup>, and is superimposed with the C=N vibration of the pyridine moiety (Fig. 2). Thus, the role of each carboxyl group differs based on the expected molecular design of EuL<sup>COOH</sup>; *i.e.* one group is free and the other coordinates to the Eu ion. The broad band at 3300–2000 cm<sup>-1</sup> in L<sup>COOH</sup> indicates intermolecular hydrogen bonds because the band is not present for EuL<sup>COOH</sup> (Fig. S1, ESI<sup>†</sup>).



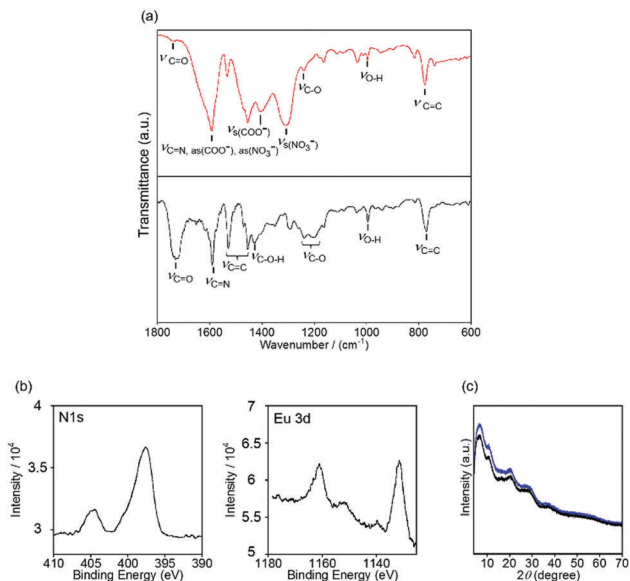


Fig. 2 (a) Attenuated total reflection FT-IR spectra of  $L^{\text{COOH}}$  (black) and  $\text{Eu}L^{\text{COOH}}$  (red). (b) XPS bands of  $\text{Eu}L^{\text{COOH}}$  and (c) synchrotron XRPD patterns of  $\text{Eu}L^{\text{COOH}}$  at rt (black) and 77 K (blue).  $\lambda = 1.00092 \text{ \AA}$ .

The ATR FT-IR bands of  $\text{Tb}L^{\text{COOH}}$  and  $\text{Gd}L^{\text{COOH}}$  are similar to those of  $\text{Eu}L^{\text{COOH}}$ , which indicates that the  $\text{Ln}L^{\text{COOH}}$  series has a similar molecular structure (Fig. S1, ESI<sup>†</sup>).

Two nitrate anions exist as counter anions to neutralize the valence of  $\text{Eu}L^{\text{COOH}}$ ;  $\text{Eu}L^{\text{COOH}}$  is estimated as a cationic component in the valence of 2+ from the FT-IR results. The N 1s XPS bands of  $\text{Eu}L^{\text{COOH}}$  appear at 404.5 and 397.6 eV and are assigned to the nitrate anions and six nitrogen atoms of  $L^{\text{COOH}}$  (Fig. 2(b)). From the ratios of their band areas, the existence ratios for the nitrate anions and six nitrogen atoms of  $L^{\text{COOH}}$  are 1 : 3. Thus, the two nitrate ions exist as counter anions and  $\text{Eu}L^{\text{COOH}}$  is the divalent cation in the solid state.

From these results, a molecular structure can be suggested (Fig. 3). Six nitrogen atoms and one carboxyl group of a  $L^{\text{COOH}}$  ligand coordinate to an Eu ion; the other carboxyl group will not coordinate. Synchrotron X-ray powder diffraction (XRPD) patterns of  $\text{Eu}L^{\text{COOH}}$  at room temperature and 77 K were obtained (Fig. 2(c)). The broadening is insufficient to assign the structure; however, the shape is reproducible at room temperature and 77 K. Thus, the crystalline phase of  $\text{Eu}L^{\text{COOH}}$  is quite low.

Electronic absorption spectra localized on the ligand of  $\text{Eu}L^{\text{COOH}}$  in the solid state are broadly observed at 300–350 nm

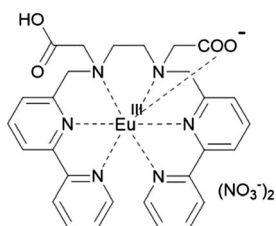


Fig. 3 Assumed molecular structure of  $\text{Eu}L^{\text{COOH}}$  in the solid state.

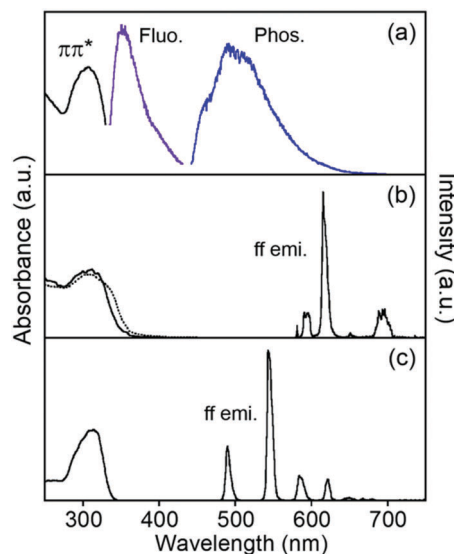


Fig. 4 Electronic absorption and luminescence spectra of  $\text{Ln}L^{\text{COOH}}$  at rt. Ln = Gd (a), Eu (b), and Tb (c) in the solid state. The phosphorescence spectrum of  $\text{Gd}L^{\text{COOH}}$  was measured at 77 K. The dotted line shows the ligand itself.  $\lambda_{\text{ex}} = 315 \text{ nm}$ .

as the  $\pi\pi^*$  transition (Fig. 4). These bands of  $\text{Tb}L^{\text{COOH}}$  and  $\text{Gd}L^{\text{COOH}}$  appear at corresponding positions.  $\text{Gd}^{\text{III}}$  complexes are convenient probes for assessing the organic electronic structure of  $L^{\text{COOH}}$ .<sup>77–79</sup> They indicate the energy of the triplet states localized on the constituting ligand because  $\text{Gd}^{\text{III}}$  possesses an accepting electronic level ( $32\,000 \text{ cm}^{-1}$ ). It is located at a sufficiently high energy to prevent any population component present on the phosphorescence spectrum. From the observation of luminescence at room temperature and 77 K in the solid state, the 350 and 455 (sh) nm bands of  $\text{Gd}L^{\text{COOH}}$  support the excited singlet and lowest triplet energy states at approximately  $28\,600$  and  $22\,000 \text{ cm}^{-1}$ , respectively (Fig. 4). The latter band appears as the shoulder of a broad phosphorescence around 490 nm.

$\text{Eu}L^{\text{COOH}}$  in the solid state at room temperature shows the ff luminescence bands of  $\text{Eu}^{\text{III}}$  at 580.3, 590 (sh), 614.4, and 650.8 nm assigned to the  $^5\text{D}_0 \rightarrow ^7\text{F}_0$ ,  $^5\text{D}_0 \rightarrow ^7\text{F}_1$ ,  $^5\text{D}_0 \rightarrow ^7\text{F}_2$ , and  $^5\text{D}_0 \rightarrow ^7\text{F}_3$  transitions, respectively ( $\lambda_{\text{ex}} = 315 \text{ nm}$ ). The broad band around 680–720 nm is assigned to the  $^5\text{D}_0 \rightarrow ^7\text{F}_4$  transition. The excitation spectrum of  $\text{Eu}L^{\text{COOH}}$  corresponds to its absorption spectrum in the solid state (Fig. S2, ESI<sup>†</sup>). This means that the  $\pi$ -electronic systems of the ligand act as photo-antennae and provide excitation energy transfer to the metal ion. The luminescence quantum yields ( $\phi_{\text{L-Ln}}$ ), lifetimes ( $\tau$ ), and photophysical data of  $\text{Eu}L^{\text{COOH}}$  are summarized in Table 1 and Fig. S3, ESI<sup>†</sup>.

The values of  $\phi_{\text{L-Ln}}$  at room temperature and 77 K are 9.1 and 18.6%, respectively. Each luminescence decay curve of  $\text{Eu}L^{\text{COOH}}$  at room temperature and 77 K can be divided into two luminescence components. This indicates that  $\text{Eu}L^{\text{COOH}}$  has at least two packing structures in the solid state.<sup>80</sup> From the equations in the ESI<sup>†</sup>, the efficiency of the energy transfer ( $\eta_{\text{EnT}}$ ) at room temperature increases and the non-radiative rate



**Table 1** Luminescence lifetimes ( $\tau_{\text{obs}}$ , amplitude), absolute luminescence quantum yields ( $\phi_{\text{L-Ln}}$ ), and photophysical data for  $\text{EuL}^{\text{COOH}}$  and  $\text{TbL}^{\text{COOH}}$  in the solid state

		$\tau_{\text{obs}}$ (ms, amp.)	$\phi_{\text{L-Ln}}^a$	$k_{\text{R}}$ ( $\text{s}^{-1}$ )	$k_{\text{NR}}$ ( $\text{s}^{-1}$ )	$\phi_{\text{L-Ln}}$ (%)	$\eta_{\text{EnT}}$ (%)
$\text{EuL}^{\text{COOH}}$	rt	0.80 (0.86) 0.40 (0.14)	9.1	500	800	39	24
	77 K	1.08 (0.57) 0.43 (0.43)	18.6	440	640	41	46
$\text{TbL}^{\text{COOH}}$	rt	0.96 (0.61) 0.40 (0.39)	10.9	—	—	—	—
	77 K	1.22 (0.56) 0.50 (0.44)	27.7	—	—	—	—

<sup>a</sup> The values for Ln emission are based on the ligand excitation.

constant ( $k_{\text{NR}}$ ) decreases with decreasing temperature, increasing the  $\phi_{\text{L-Ln}}$  value at 77 K.  $\text{TbL}^{\text{COOH}}$  also shows luminescence in the green wavelength region. The luminescence bands of  $\text{TbL}^{\text{COOH}}$  in the solid state appeared at 490.0, 542.4, 584.4, 622.1, 649.2, 667.9, and 680.9 nm, and are assigned to the  $^5\text{D}_4 \rightarrow ^7\text{F}_6$ ,  $^5\text{D}_4 \rightarrow ^7\text{F}_5$ ,  $^5\text{D}_4 \rightarrow ^7\text{F}_4$ ,  $^5\text{D}_4 \rightarrow ^7\text{F}_3$ ,  $^5\text{D}_4 \rightarrow ^7\text{F}_2$ ,  $^5\text{D}_4 \rightarrow ^7\text{F}_1$ , and  $^5\text{D}_4 \rightarrow ^7\text{F}_0$  transitions, respectively. The excitation spectrum of  $\text{TbL}^{\text{COOH}}$  in the solid state also corresponds to its absorption spectrum (Fig. S2, ESI<sup>†</sup>). The values of  $\phi_{\text{L-Ln}}$  at room temperature and 77 K are 10.9 and 27.7%, respectively. There are two luminescence components at room temperature and 77 K, which is the same as that observed for  $\text{EuL}^{\text{COOH}}$  (Table 1).

The assumed energy diagram is shown in Fig. 5. The singlet and triplet levels localized on  $\text{L}^{\text{COOH}}$  are estimated from the results for  $\text{GdL}^{\text{COOH}}$ , as described above.  $\text{EuL}^{\text{COOH}}$  shows ff luminescence *via* the intramolecular energy transfer from the triplet state after the intersystem crossing of the excited singlet in  $\text{L}^{\text{COOH}}$ . The ff emissions of  $\text{Tb}^{\text{III}}$  often show thermal sensitivity because of the thermal equilibrium between the energy donor and acceptor level.<sup>81,82</sup> In our previous report, the parent  $\text{TbL}$  molecule showed negligibly weak ff emissions (1%) at room temperature, but efficient emissions (>90%) at 77 K because of the thermal equilibrium between the triplet state of  $\text{L}$  (21 700  $\text{cm}^{-1}$ ) and an acceptor level ( $^5\text{D}_4$ ; 20 500  $\text{cm}^{-1}$ ) of  $\text{Tb}$ .<sup>83</sup> Thus,  $\text{L}^{\text{COOH}}$  acts as a more efficient energy donor to  $\text{Tb}$  than  $\text{L}$ . Furthermore, the luminescence intensity of  $\text{TbL}^{\text{COOH}}$  increases at 77 K because the energy transfer accelerates toward the central metal. The value of  $\text{TbL}^{\text{COOH}}$  is lower than that of  $\text{TbL}$

at 77 K, indicating that it is enhanced by the different intermolecular interactions. The complexes with  $\text{L}^{\text{COOH}}$  also show amorphous-like XRPD patterns (Fig. 2(c)).

## 2.2 Structure and luminescence of $\text{LnL}^{\text{COOH}}$ in an aqueous solution

### 2.2.1 Luminescence of $\text{EuL}^{\text{COOH}}$ , $\text{GdL}^{\text{COOH}}$ , and $\text{TbL}^{\text{COOH}}$

The electronic absorption spectra of the  $\text{EuL}^{\text{COOH}}$  and the  $\text{L}^{\text{COOH}}$  ligands in aqueous solution are shown in Fig. 6. The absorption bands of  $\text{L}^{\text{COOH}}$  in  $\text{H}_2\text{O}$  appear at 289, 299, and 315 (sh) nm.  $\text{EuL}^{\text{COOH}}$  in  $\text{H}_2\text{O}$  shows bands at 305 and 315 (sh) nm, which are assigned to the  $\pi\pi^*$  transitions and correspond well with those in  $\text{D}_2\text{O}$ . The band position of  $\text{EuL}^{\text{COOH}}$  in  $\text{H}_2\text{O}$  or  $\text{D}_2\text{O}$  appears at a lower transition energy than that of the  $\text{L}^{\text{COOH}}$  ligand. This indicates that the ligand surrounds an Eu ion through coordination bonds in  $\text{H}_2\text{O}/\text{D}_2\text{O}$ , and forms a  $\pi$ -conjugation configuration that is longer than the ligand itself. The  $\pi\pi^*$  electronic absorption bands of  $\text{TbL}^{\text{COOH}}$  and  $\text{GdL}^{\text{COOH}}$  in water also appear at the same positions as those of  $\text{EuL}^{\text{COOH}}$  (Fig. 6). The triplet state as an energy donor level for the lanthanide complex with  $\text{L}^{\text{COOH}}$  in solution was also estimated at approximately 22 800  $\text{cm}^{-1}$  from the phosphorescence band (438 nm) of  $\text{GdL}^{\text{COOH}}$  in ethanol at 77 K, which is the same as that in the

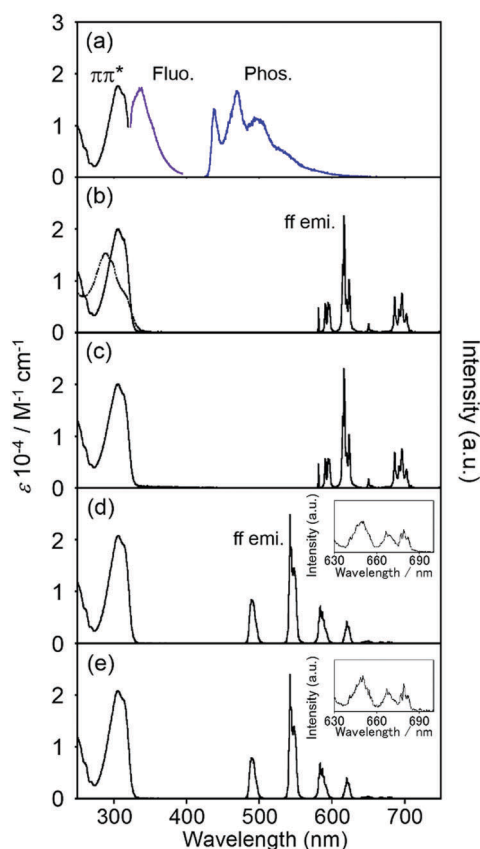


**Fig. 6** Electronic absorption and luminescence spectra of  $\text{GdL}^{\text{COOH}}$  in aqueous solution (a). A phosphorescence band was observed in ethanol at 77 K. Electronic absorption and ff emission spectra of  $\text{EuL}^{\text{COOH}}$  and  $\text{TbL}^{\text{COOH}}$  in  $\text{H}_2\text{O}$  (b and d) and  $\text{D}_2\text{O}$  (c and e).  $\lambda_{\text{ex}} = 315$  nm. The inset shows the extended view.

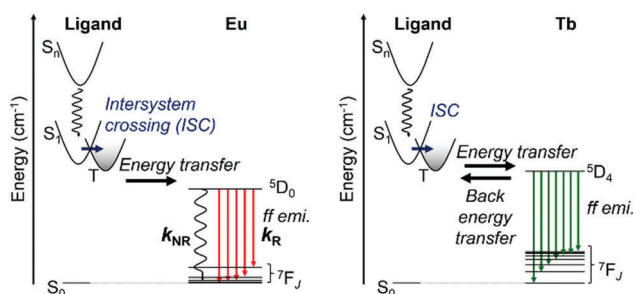


**Fig. 5** Schematic representation of energy diagram of  $\text{EuL}^{\text{COOH}}$  (left) and  $\text{TbL}^{\text{COOH}}$  (right) in the solid state.



**Table 2** Luminescence lifetimes ( $\tau_{\text{obs}}$ , amplitude), absolute luminescence quantum yields ( $\phi_{\text{L-Ln}}$ ), and photophysical data for  $\text{EuL}^{\text{COOH}}$  and  $\text{TbL}^{\text{COOH}}$  in  $\text{H}_2\text{O}$  and  $\text{D}_2\text{O}$

		$\tau_{\text{obs}}$ (ms, amp.)	$\phi_{\text{L-Ln}}^a$	$k_{\text{R}}$ ( $\text{s}^{-1}$ )	$k_{\text{NR}}$ ( $\text{s}^{-1}$ )	$\phi_{\text{L-Ln}}$ (%)	$\eta_{\text{EnT}}$ (%)
$\text{EuL}^{\text{COOH}}$	$\text{H}_2\text{O}$	0.57 (1.00)	11.5	250	1500	14	76
	$\text{D}_2\text{O}$	1.94 (1.00)	35.4	250	270	49	74
$\text{TbL}^{\text{COOH}}$	$\text{H}_2\text{O}$	1.50 (1.00)	51.6	—	—	—	—
	$\text{D}_2\text{O}$	2.41 (1.00)	81.6	—	—	—	—

<sup>a</sup> The values of Ln emission are based on the ligand excitation.

solid state (Fig. 6(a)). The band position in the solid state shifted toward the blue in the protic solvent. The band shape in solution became sharper than that in the solid state. The different energy donor levels for the solid state in solution particularly affect the luminescence properties of  $\text{TbL}^{\text{COOH}}$  (*vide infra*). The fluorescence band of  $\text{GdL}^{\text{COOH}}$  in aqueous solution appears at 336 nm.

The luminescence spectra and photophysical data of  $\text{EuL}^{\text{COOH}}$  in  $\text{H}_2\text{O}$  and  $\text{D}_2\text{O}$  are shown in Fig. 6 and Table 2. The luminescence bands of  $\text{EuL}^{\text{COOH}}$  in  $\text{H}_2\text{O}/\text{D}_2\text{O}$  sharply appear at 580.5, 594.2, 615.9, 649.7, and 680–720 nm, and are assigned to the ff transitions. The Stark splitting of  $\text{EuL}^{\text{COOH}}$  in  $\text{H}_2\text{O}$  and  $\text{D}_2\text{O}$  differs from that in the solid state because of the differences of ligand fields. The excitation spectrum of  $\text{EuL}^{\text{COOH}}$  corresponds to its absorption spectrum (Fig. S4, ESI<sup>†</sup>).

From the luminescence decay profile measurement,  $\text{EuL}^{\text{COOH}}$  in  $\text{H}_2\text{O}$  and  $\text{D}_2\text{O}$  has a single luminescence component with lifetimes of 0.57 and 1.94 ms, respectively (Table 2 and Fig. S5, ESI<sup>†</sup>). The value of  $\phi_{\text{L-Ln}}$  in  $\text{H}_2\text{O}$  is 11.5%, which is relatively higher than that in the solid state (Table 1). The quantum yield of  $\text{EuL}$  in acetonitrile is lower than that in the solid state.<sup>73</sup> The value of  $\phi_{\text{L-Ln}}$  in  $\text{D}_2\text{O}$  is 35.4%. It is caused by the deuterium effect because the five-fold vibrational mode in  $\text{D}_2\text{O}$  affects the excited state of  $\text{Eu}^{\text{III}}$  less than the three-fold vibrational mode in  $\text{H}_2\text{O}$ .<sup>84–92</sup> The value of  $\phi_{\text{L-Ln}}$  and the lifetime of the Eu complex in  $\text{D}_2\text{O}$  seem larger than those in  $\text{H}_2\text{O}$ . The radiation and non-radiation rate constants are 250 and 270  $\text{s}^{-1}$  in  $\text{D}_2\text{O}$ , respectively, while those in  $\text{H}_2\text{O}$  are 250 and 1500  $\text{s}^{-1}$ , respectively. Application of Horrocks' equation to the observed luminescence lifetimes in water is a useful method for understanding the molecular structure of Eu complexes because of the estimation method that is used for the number of coordinating water molecules.<sup>93–95</sup>

The  $q$  value represents the number of water molecules and is calculated by the following equation:

$$q = 1.11[\tau_{\text{H}_2\text{O}}^{-1} - \tau_{\text{D}_2\text{O}}^{-1} - 0.31] \quad (1)$$

where  $\tau_{\text{H}_2\text{O}}$  and  $\tau_{\text{D}_2\text{O}}$  are the luminescence lifetimes of ff emission in  $\text{H}_2\text{O}$  and  $\text{D}_2\text{O}$ , respectively. Thus, the number of coordinating water molecules to an Eu ion is calculated as 1.0 in  $\text{EuL}^{\text{COOH}}$ , which indicates that one water molecule will bind to each Eu ion in  $\text{EuL}^{\text{COOH}}$ .

The luminescence band shapes of  $\text{TbL}^{\text{COOH}}$  in  $\text{H}_2\text{O}$  and  $\text{D}_2\text{O}$  are sharper than that in the solid state, which is the same as that observed for  $\text{EuL}^{\text{COOH}}$  (Fig. 6). The luminescence bands of

$\text{TbL}^{\text{COOH}}$  in  $\text{H}_2\text{O}/\text{D}_2\text{O}$  are observed at 490.1, 541.6, 584.0, 621.4, 650.4, 668.7, and 679.8 nm, and are assigned to the  $^5\text{D}_4 \rightarrow ^7\text{F}_6$ ,  $^5\text{D}_4 \rightarrow ^7\text{F}_5$ ,  $^5\text{D}_4 \rightarrow ^7\text{F}_4$ ,  $^5\text{D}_4 \rightarrow ^7\text{F}_3$ ,  $^5\text{D}_4 \rightarrow ^7\text{F}_2$ ,  $^5\text{D}_4 \rightarrow ^7\text{F}_1$ , and  $^5\text{D}_4 \rightarrow ^7\text{F}_0$  transitions, respectively. The excitation spectrum of  $\text{TbL}^{\text{COOH}}$  also corresponds to its absorption spectrum (Fig. S4, ESI<sup>†</sup>). The  $\phi_{\text{L-Ln}}$  values of  $\text{TbL}^{\text{COOH}}$  in  $\text{H}_2\text{O}$  and  $\text{D}_2\text{O}$  are 51.6% and 81.6%, respectively. Interestingly, these values are much higher than the values in the solid state. As discussed above, the phosphorescence band has a vibrational structure, and the level of the lowest triplet state in solution is higher than that in the solid state. Thus, the energy transfer in  $\text{TbL}^{\text{COOH}}$  occurs more efficiently in  $\text{H}_2\text{O}$  or  $\text{D}_2\text{O}$ . The luminescence decay profile of  $\text{TbL}^{\text{COOH}}$  shows a single component in both  $\text{H}_2\text{O}$  and  $\text{D}_2\text{O}$ . The number of coordinating water molecules of  $\text{TbL}^{\text{COOH}}$  in water are also estimated by Horrocks' equation:<sup>93,94</sup>

$$q = 4.2 [\tau_{\text{H}_2\text{O}}^{-1} - \tau_{\text{D}_2\text{O}}^{-1}] \quad (2)$$

The calculated number of coordination water molecules is 1.1. This value corresponds to that of  $\text{EuL}^{\text{COOH}}$  in  $\text{H}_2\text{O}$ , which indicates that the coordination environments are similar to each other.

Generally, the molecular shape, including the coordination sphere of metal complexes in water, should be considered for the molecular design along with several methods under presumable structural viewpoints. From the ESI-MS measurement,  $\text{EuL}^{\text{COOH}}$ ,  $\text{GdL}^{\text{COOH}}$ , and  $\text{TbL}^{\text{COOH}}$  in aqueous solution are detected at their expected mass number (Fig. S6, ESI<sup>†</sup>). The assumed structure of  $\text{EuL}^{\text{COOH}}$  in aqueous solution is shown in Fig. 7. There are three possibilities to form a complex: structure A has two carboxylate groups that are bound to the Eu ion with the six nitrogen atoms of the ligand, structure C has both carboxylic groups released from the Eu ion, and structure B has one carboxylate coordinated to the metal ion and the other is released. It is impossible to combine more water molecules for structure A, while structure C is able to take on more than two water molecules. However, structure B has an open site to coordinate one water molecule.  $\text{Eu}/\text{Tb}$  has a suitable  $q$  value from the viewpoint of steric hindrance for the  $\text{Eu}/\text{TbL}^{\text{COOH}}$  complex, which is eight-coordinated by  $\text{L}^{\text{COOH}}$  and  $\text{H}_2\text{O}$  based on the molecular structure assumed from the FT-IR spectra of structure B. That is, it strongly suggests that one carboxyl group of  $\text{Eu}/\text{TbL}^{\text{COOH}}$  will be released for water solubility, opening the water coordination to Eu.

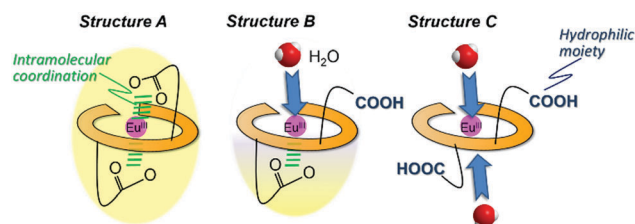


**Fig. 7** Assumed structures in aqueous solution of  $\text{EuL}^{\text{COOH}}$ . The ligand  $\pi$  electronic system is shown in yellow. (a) an insoluble form due to the two intramolecular COO group coordination to Eu, (b) a half  $\text{H}_2\text{O}$ -accessible form with an intramolecular COO group coordination to Eu, and (c) a water-soluble and  $\text{H}_2\text{O}$ -accessible form from both apical sites.



### 2.2.2 pH dependence on the luminescence of $\text{EuL}^{\text{COOH}}$

Based on the previous section, a carboxylate or carboxylic acid moiety that does not combine with the Eu ion during complex formation will act as a weak acid in water. The pH value of a  $5.0 \times 10^{-5} \text{ mol cm}^{-3}$  aqueous solution of  $\text{EuL}^{\text{COOH}}$  is 4.05, and the acid dissociation constant ( $\text{pK}_a$ ) is calculated as 3.91. From the comparison of the values of the ligand itself, the pH value is 4.09 at  $5.0 \times 10^{-5} \text{ mol cm}^{-3}$ , thus the notable acidity of an aqueous  $\text{EuL}^{\text{COOH}}$  solution is caused by the carboxylate released from Eu, as well as factors discussed in Fig. 7.

The electronic absorption and luminescence spectra in aqueous solutions at various pH values are shown in Fig. 8. The absorption and luminescence band shapes of  $\text{EuL}^{\text{COOH}}$  do not change at pH 9.7. The value of  $\phi_{\text{L-Ln}}$  and the luminescence lifetime of  $\text{EuL}^{\text{COOH}}$  at pH 9.7 are 10.6% and 0.57 ms, respectively. Thus, the molecular structure and coordination environment surrounding Eu are extremely stable at pH = 4.0–9.7.

As the pH increases above 10.4, the major electronic absorption band at 305 nm (observed at pH 9.7) gradually shifts to a higher energy, and appears at 302 nm at pH 11.9. In contrast, the band positions and shapes of the ff emissions drastically change when the pH changes from 9.7 to 11.9 (Fig. 8). Two luminescence components are observed in the luminescence decay profile at pH 10.4, indicating that the molecular structure of  $\text{EuL}^{\text{COOH}}$  at pH 10.4 differs from that in the initial state (Fig. S7, ESI<sup>†</sup>). The luminescence lifetimes of  $\text{EuL}^{\text{COOH}}$  in  $\text{H}_2\text{O}$  under basic conditions are estimated to be 0.36 ms (amplitude 0.92) and 0.83 ms (0.08), and that in  $\text{D}_2\text{O}$  is estimated to be 1.75 ms (Fig. S8, ESI<sup>†</sup>). Based on these major values,  $\text{EuL}^{\text{COOH}}$  will change its molecular structure under basic conditions while maintaining the coordination between Eu and  $\text{L}^{\text{COOH}}$  (Fig. S9(a), ESI<sup>†</sup>); the carboxylate group or a part of the pyridine moiety will be released from the Eu ion because of the increasing  $q$  value compared to that for the initial condition (ESI<sup>†</sup>). This also shows the reversibility of the electronic absorption and luminescence spectra at pH 3.5 using hydrochloric acid, indicating that  $\text{EuL}^{\text{COOH}}$  demonstrates a stable and flexible molecular change at alkaline pH (Fig. S10, ESI<sup>†</sup>).

The electronic absorption and luminescence spectra in an acidic aqueous solution are shown in Fig. 9. The absorption spectra of  $\text{EuL}^{\text{COOH}}$  shift to slightly shorter wavelengths by 2 nm after adjustment with hydrochloric acid compared to

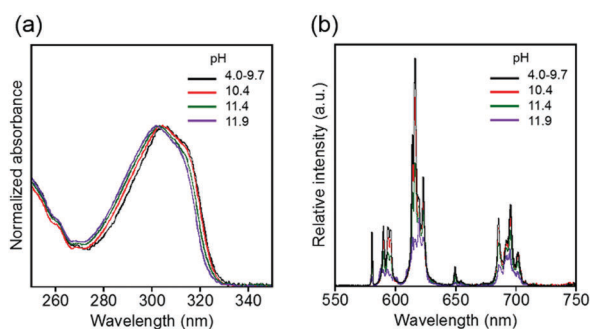


Fig. 8 pH dependence of electronic absorption (a) and luminescence (b) spectra of  $\text{EuL}^{\text{COOH}}$  in the pH region of 4.0–11.9.  $\lambda_{\text{ex}} = 315 \text{ nm}$ .

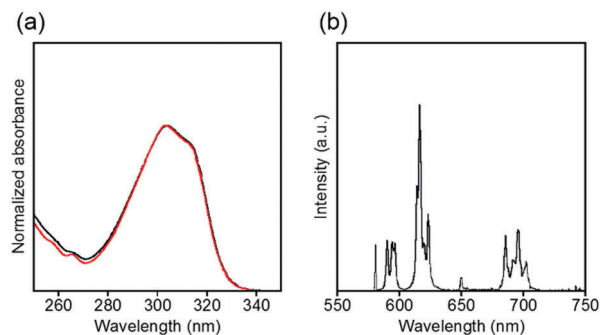
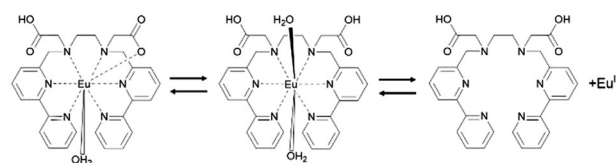


Fig. 9 Electronic absorption (a) and luminescence (b) spectra of  $\text{EuL}^{\text{COOH}}$  in acidic aqueous solutions. The black and red lines show a pH of 2.6 and 1.9–2.1, respectively.  $\lambda_{\text{ex}} = 315 \text{ nm}$ .

the initial solution. The luminescence bands of  $\text{EuL}^{\text{COOH}}$  correspond in the pH region of 4.0–2.6, but the intensities become weaker and are finally quenched below pH 1.9 (Fig. S11, ESI<sup>†</sup>). The absorption spectra of  $\text{EuL}^{\text{COOH}}$  under acidic conditions correspond to that of  $\text{L}^{\text{COOH}}$  under the same pH conditions (Fig. S12, ESI<sup>†</sup>), meaning that  $\text{EuL}^{\text{COOH}}$  will be decomposed by the strong acidic condition. These results are well supported by the ESI-MS data shown in Fig. 8(b)–(d); in particular, the  $m/z$  values of 257.2 and 513.3 observed at pH 1.9 can be assigned to the diprotonated and monoprotonated species of  $\text{L}^{\text{COOH}}$ . Adjusting the pH toward the initial value causes the absorption and luminescence bands to reproduce their positions and intensities, indicating that  $\text{EuL}^{\text{COOH}}$  has a surprising ability to re-coordinate (Fig. S13, ESI<sup>†</sup>).

Luminescence lifetimes in  $\text{H}_2\text{O}$  and  $\text{D}_2\text{O}$  were observed in an acidic solution to examine the process of luminescence quenching of  $\text{EuL}^{\text{COOH}}$  (Fig. S14, ESI<sup>†</sup>). The luminescence lifetimes of the luminescent component for  $\text{EuL}^{\text{COOH}}$  in  $\text{H}_2\text{O}$  and  $\text{D}_2\text{O}$  under acidic conditions are 0.42 and 2.22 ms, respectively. The  $q$  value in the acidic solution is estimated as 1.7 for  $\text{EuL}^{\text{COOH}}$ . This value is higher than that under initial conditions. Additionally, each solution shows a second luminescence component with a relatively short lifetime ( $< 0.01 \text{ ms}$ ), which is assigned to the dissociation of  $\text{EuL}^{\text{COOH}}$ . This suggests that two water molecules will coordinate to Eu around pH 2, and the dissociated complex partly exists in this equilibrium. The absolute luminescence quantum yield is 0.2% at pH 2.1.

From the above results, the assumed dissociation process of  $\text{EuL}^{\text{COOH}}$  in aqueous solutions is shown in Scheme 1. One carboxylate coordinates to the Eu ion and the other exists as carboxylic acid; a water molecule binds to the central metal at pH = 2.6–9.7. With decreasing pH values, two water molecules bind to the Eu ion, the carboxylate releases from the Eu ion,



Scheme 1 Assumed dissociation process of  $\text{EuL}^{\text{COOH}}$  in aqueous solution.



and  $\text{EuL}^{\text{COOH}}$  dissociates at pH 1.9 with protonation of the  $\text{L}^{\text{COOH}}$  ligand. These molecular structural changes are readily reversible.

### 3. Conclusions

The photophysical behaviour and structure of a water-soluble Eu complex with  $\text{L}^{\text{COOH}}$ , based on the helicate structure and functional carboxylate, were examined in aqueous solution at various pH values. The coordination number of the Eu complex  $\text{EuL}^{\text{COOH}}$  was assumed to be greater than 8. One of the two carboxylate groups is released from the Eu ion, even in the powdered state, while the other carboxylate acts to provide hydrophilicity in water.  $\text{EuL}^{\text{COOH}}$  shows ff luminescence in the solid state. This molecule keeps the ff emission of Eu in the wide pH range of 2.6–9.7, and shows spectral reversibility at pH = 1.9–11.9. The luminescence lifetimes of  $\text{EuL}^{\text{COOH}}$  in  $\text{H}_2\text{O}$  and  $\text{D}_2\text{O}$  make it possible to estimate the number of coordinated water molecules to Eu as 1 at the initial condition (pH = 2.6–9.7). In both strongly basic and strongly acidic conditions, this value increases with molecular structural changes. For instance, one carboxyl group binding to Eu will release from Eu at approximately pH = 2.1–2.6. Furthermore,  $\text{EuL}^{\text{COOH}}$  completely decomposes below pH 1.9 and recovers as a complex with adjustments toward the initial pH.  $\text{TbL}^{\text{COOH}}$  also shows luminescence in the green wavelength region for ff emission, and a water molecule is combined with the Tb ion in the initial condition. The luminescence quantum yield of  $\text{TbL}^{\text{COOH}}$  in  $\text{H}_2\text{O}$  is higher than that in the solid state. The luminescence mechanisms of  $\text{EuL}^{\text{COOH}}$  and  $\text{TbL}^{\text{COOH}}$  are discussed based on the energy relaxation process of the triplet state of the  $\text{L}^{\text{COOH}}$  ligand of  $\text{GdL}^{\text{COOH}}$ .

## 4. Experimental

### 4.1 Regents and materials

Commercially available reagents and spectral-grade solvents (Wako Pure Chemical Industries Ltd, Tokyo Chemical Industry Ltd, and Kanto Chemical Co. Inc.) were generally used without further purification. Water was purified using a Direct-Q3 UV-Remote Water Purification System (Merck Millipore). Preparative layer chromatography was performed using silica (Merck silica gel 60, 2 mm). The concentration of the measured sample was  $3.0 \times 10^{-5}$  M. The pH values were adjusted by the addition of sodium hydroxide or hydrochloric acid.

### 4.2 Syntheses

**4.2.1  $N^1, N^2$ -Bis([2,2'-bipyridin]-6-ylmethyl)ethane-1,2-diamine (LH).** The starting chemical, L, was synthesized as previously reported.<sup>73</sup> For the synthesis of LH, L (79.4 mg, 0.202 mmol) and sodium borohydride (100 mg, 2.64 mmol) were dissolved in methanol (100 mL), and the mixture was stirred for 1 day. The solvent mixture was evaporated to dryness. The crude residue was dissolved in  $\text{CHCl}_3/\text{H}_2\text{O}$ , and the organic phase was extracted. The extract was dried with  $\text{MgSO}_4$ . The yellow oil

product was obtained from the solution by filtration; it was washed with chloroform and dried under vacuum. Yield: 77.3 mg (96%).  $^1\text{H-NMR}$  (500.00 MHz,  $\text{CDCl}_3$ , Fig. S15, ESI<sup>+</sup>);  $\delta$  8.65 (d, 2H), 8.40 (d, 2H), 8.26 (d, 2H), 7.43 (m, 4H), 7.29 (q, 4H), 4.01 (s, 4H), 2.93 (s, 4H). MS (FAB<sup>+</sup>);  $m/z$ , 397 [ $\text{M} + \text{H}$ ]<sup>+</sup> (calcd 397.50).

**4.2.2 Diethyl 2,2'-(ethane-1,2-diylbis([2,2'-bipyridin]-6-ylmethyl)azanediyl)diacetate ( $\text{L}^{\text{COOEt}}$ ).** LH (38.0 mg, 95.8  $\mu\text{mol}$ ) was dissolved in acetonitrile and stirred with potassium carbonate (0.50 g, 3.6 mmol). Then, ethyl bromoacetate (0.30 g, 1.8 mmol) was added to the solution and stirred for 2 h under an argon atmosphere. The product was purified by preparative layer chromatography ( $\text{CH}_2\text{Cl}_2/\text{methanol}$ , 40:1). Yield: 33.8 mg (62%).  $^1\text{H-NMR}$  (500.00 MHz,  $\text{CDCl}_3$ , Fig. S16, ESI<sup>+</sup>)  $\delta$  8.65 (d, 2H), 8.38 (d, 2H), 8.23 (d, 2H), 7.75 (m, 4H), 7.49 (d, 2H), 7.28 (m, 4H), 4.04 (s, 4H), 3.52 (s, 4H), 3.20 (m, 6H), 2.96 (s, 4H) MS (FAB<sup>+</sup>);  $m/z$ , 569 [ $\text{M} + \text{H}$ ]<sup>+</sup> (calcd 569.68).

**4.2.3 2,2'-(Ethane-1,2-diylbis([2,2'-bipyridin]-6-ylmethyl)azanediyl)diacetic acid ( $\text{L}^{\text{COOH}}$ ).**  $\text{L}^{\text{COOEt}}$  was dissolved in ethanol (15 mL), and the pH was adjusted to 12 using 5 N NaOH. After stirring for 2 h, the solvent mixture was adjusted to pH 5 using 6 N HCl. The white powder product was obtained by evaporation to dryness and extraction with ethanol. Yield: 14.9 mg (49%).  $^1\text{H-NMR}$  (500.00 MHz,  $\text{methanol-d}_4$ , Fig. S17, ESI<sup>+</sup>); 8.89 (d, 2H), 8.72 (d, 2H), 8.63 (t, 2H), 8.36 (d, 2H), 8.09 (m, 4H), 7.72 (d, 2H), 4.59 (s, 4H), 4.01 (s, 4H), 3.66 (s, 4H); MS (FAB<sup>+</sup>);  $m/z$ , 513 [ $\text{M} + \text{H}$ ]<sup>+</sup> (calcd 513.57).

**4.2.4  $\text{EuL}^{\text{COOH}}$ .**  $\text{Eu}(\text{NO}_3)_3 \cdot 6\text{H}_2\text{O}$  (17.0 mg, 38.1  $\mu\text{mol}$ ) in ethanol (5 mL) was slowly added to a solution of  $\text{L}^{\text{COOH}}$  (18.4 mg, 35.9  $\mu\text{mol}$ ) in ethanol (5 mL). After stirring for 24 h, the white precipitate was filtered and washed with ethanol. The complex was characterized by FT-IR and ESI-MS. Yield 18.7 mg (72%); ESI-MS [ $\text{M} - (\text{NO}_3^-)_2 - \text{H}^+$ ]<sup>+</sup>  $m/z$  = 663.2 (calcd 662.52).

**4.2.5  $\text{GdL}^{\text{COOH}}$ .**  $\text{Gd}(\text{NO}_3)_3 \cdot 5\text{H}_2\text{O}$  (30.4 mg, 67.4  $\mu\text{mol}$ ) in ethanol (5 mL) was slowly added to a solution of  $\text{L}^{\text{COOH}}$  (25.2 mg, 49.3  $\mu\text{mol}$ ) in ethanol (5 mL). After stirring for 24 h, the white precipitate was filtered and washed with ethanol. Yield 21.5 mg (55%); ESI-MS [ $\text{M} - (\text{NO}_3^-)_2 - \text{H}^+$ ]<sup>+</sup>  $m/z$  = 668.1 (calcd 667.80).

**4.2.6  $\text{TbL}^{\text{COOH}}$ .**  $\text{Tb}(\text{NO}_3)_3 \cdot 6\text{H}_2\text{O}$  (29.5 mg, 65.1  $\mu\text{mol}$ ) in ethanol (5 mL) was slowly added to a solution of  $\text{L}^{\text{COOH}}$  (30.0 mg, 58.6  $\mu\text{mol}$ ) in ethanol (5 mL). After stirring for 24 h, the white precipitate was filtered and washed with ethanol. Yield 20.3 mg (51%); ESI-MS [ $\text{M} - (\text{NO}_3^-)_2 - \text{H}^+$ ]<sup>+</sup>  $m/z$  = 669.1 (calcd 669.13).

### 4.3 Instrumentation

$^1\text{H-NMR}$  spectra were recorded on a JEOL JMN-500II spectrometer in  $\text{CDCl}_3$  with tetramethylsilane and in  $\text{methanol-d}_4$ . ATR FT-IR spectra were measured using a Nicolet iS5 spectrometer (Thermo Scientific). XPS measurements were performed on a KRATOS AXIS ULTRA DLD (Shimadzu) equipped with a monochromatic Al-K $\alpha$  X-ray source (1253.6 eV); the binding energies were calibrated at the Au 4f level (84.0 eV). Synchrotron XRPD patterns were recorded on a large Debye-Scherrer camera installed at SPring-8 BL02B2 (JASRI/SPring-8) using an imaging



plate as a detector.<sup>96</sup> Fast atom bombardment mass spectrometry (FAB-MS) was performed using the MStation JMS-700A (JEOL). ESI-MS spectra were recorded using liquid chromatography-mass spectrometry (LC-MS 2020, Shimadzu). Electronic absorption spectra in the solid state and in solution were obtained using the diffused reflection method with conversion of the y-axis by UV-3100 and UV-3600S (Shimadzu), respectively. Luminescence and excitation spectra were recorded on a Fluorolog 3-22 (Horiba Jobin Yvon). Absolute luminescence quantum yields and luminescence lifetimes were determined using an absolute luminescence quantum yield C9920-02 spectrometer (Hamamatsu Photonics K. K.) and a QuantaTaurus-Tau C11367-12 spectrometer (Hamamatsu Photonics K. K.), respectively, with pulsed excitation light sources. The pH values were measured using a pH meter with a freshly calibrated 3.3 M KCl electrode from DKK-TOA Corporation.

## Acknowledgements

The synchrotron radiation experiments were performed at the BL02B2 of SPring-8 with the approval of the Japan Synchrotron Radiation Research Institute (Proposal No. 2017A1648, 2016B1342, 2016B1706, 2016A1336, 2016A1333, 2014B1316, 2013B1776, 2013B1679, and 2013A1020). The ESI-MS measurements were supported by Mr Takahiro Goda at Shimadzu Corporation. This work was partly supported by the Grants-in-Aid for Scientific Research on Innovative Areas of "Element-Block Polymers (Area Number: 2401)" (No. 25107730; MH), Challenging Exploratory Research Center Project for Private University, a matching fund subsidy from MEXT (2013–2017; MH), and a SOKEN Project provided by the Aoyama Gakuin University Research Institute (2016–2017; MH). MH also acknowledges the Izumi Science and Technology Foundation for their financial support.

## References

- 1 S. V. Eliseeva and J.-C. G. Bünzli, *Chem. Soc. Rev.*, 2010, **39**, 189.
- 2 S. J. Butler and D. Parker, *Chem. Soc. Rev.*, 2013, **42**, 1652.
- 3 I. Hemmilä and V.-M. Mukkala, *Crit. Rev. Clin. Lab. Sci.*, 2001, **38**, 441.
- 4 D. Parker, *Coord. Chem. Rev.*, 2000, **205**, 109.
- 5 J.-C. G. Bünzli, *Chem. Lett.*, 2009, **38**, 104.
- 6 J.-C. G. Bünzli, *J. Lumin.*, 2016, **170**, 866.
- 7 J.-C. G. Bünzli and S. V. Eliseeva, *Chem. Sci.*, 2013, **4**, 1939.
- 8 S. V. Eliseeva and J.-C. G. Bünzli, *New J. Chem.*, 2011, **35**, 1165.
- 9 M. Sy, A. Nonat, N. Hildebrandt and L. J. Charbonnière, *Chem. Commun.*, 2016, **52**, 5080.
- 10 M. V. Butovski and R. Kempe, *New J. Chem.*, 2015, **39**, 7544.
- 11 S. J. Butler and D. Parker, *Chem. Soc. Rev.*, 2013, **42**, 1652.
- 12 S. Shinoda and H. Tsukube, *Analyst*, 2011, **136**, 431.
- 13 T. Gunnlaugsson and J. P. Leonard, *Chem. Commun.*, 2005, 3114.
- 14 W. L. Scaff, Jr., D. L. Dyer and K. Mori, *J. Bacteriol.*, 1969, **98**, 246.
- 15 E. J. Soini, L. J. Pelliniemi, I. A. Hemmilä, V.-M. Mukkala, J. J. Kankare and K. Fröjdman, *J. Histochem. Cytochem.*, 1988, **36**, 1449.
- 16 S. Quici, A. Casoni, F. Foschi, L. Armelao, G. Bottaro, R. Seraglia, C. Bolzati, N. Salvarese, D. Carpanese and A. Rosato, *J. Med. Chem.*, 2015, **58**, 2003.
- 17 E. M. Rodríguez, N. Bogdan, J. A. Capobianco, S. Orlandi, M. Cavazzini, C. Scalera and S. Quici, *Dalton Trans.*, 2013, **42**, 9453.
- 18 F. Secundo, M. A. Bacigalupo, C. Scalera and S. Quici, *J. Food Compos. Anal.*, 2012, **25**, 221.
- 19 D. Kovacs, X. Li, L. S. Mészáros, M. Ott, J. Andres and K. E. Borbas, *J. Am. Chem. Soc.*, 2017, **139**, 5756.
- 20 M. Halim, M. S. Tremblay, S. Jockusch, N. J. Turro and D. Sames, *J. Am. Chem. Soc.*, 2007, **129**, 7704.
- 21 E. Pershagen, J. Nordholm and K. E. Borbas, *J. Am. Chem. Soc.*, 2012, **134**, 9832.
- 22 K. E. Borbas and J. I. Bruce, *Org. Biomol. Chem.*, 2007, **5**, 2274.
- 23 E. Pershagen and K. E. Borbas, *Angew. Chem., Int. Ed.*, 2015, **54**, 1787.
- 24 T. Terai, K. Kikuchi, Y. Urano, H. Kojima and T. Nagano, *Chem. Commun.*, 2012, **48**, 2234.
- 25 T. Terai, H. Ito, K. Kikuchi and T. Nagano, *Chem. – Eur. J.*, 2012, **18**, 7377.
- 26 S. Mizukami, T. Yamanoto, A. Yoshimura, S. Watanabe and K. Kikuchi, *Angew. Chem., Int. Ed.*, 2011, **50**, 8750.
- 27 A. T. Bui, M. Beyler, Y.-Y. Liao, A. Grichine, A. Duperray, J.-C. Mulatier, B. L. Guennic, C. Andraud, O. Maury and R. Tripiet, *Inorg. Chem.*, 2016, **55**, 7020.
- 28 S. Nadella, P. M. Selvakumar, E. Suresh, P. S. Subramanian, M. Albrecht, M. Giese and R. Fröhlich, *Chem. – Eur. J.*, 2012, **18**, 16784.
- 29 A. Mohamadi and L. W. Miller, *Bioconjugate Chem.*, 2016, **27**, 2540.
- 30 G. L. Law, R. Pal, L. O. Palsson, D. Parker and K.-L. Wong, *Chem. Commun.*, 2009, 7321.
- 31 J. R. Diniz, J. R. Correa, D. de A. Moreira, R. S. Fontenele, A. L. de Oliveira, P. V. Abdelnur, J. D. L. Dutra, R. O. Freire, M. O. Roderigues and B. A. D. Neto, *Inorg. Chem.*, 2013, **52**, 10199.
- 32 B. T. Nguyen, A. J. Ingram and G. Muller, *Chemistry*, 2016, **28**, 325.
- 33 T. Uchida, K. Nozaki and M. Iwamura, *Chem. – Asian J.*, 2016, **11**, 2415.
- 34 R. A. Poole, G. Bobba, M. J. Cann, J.-C. Frias, D. Parker and R. D. Peacock, *Org. Biomol. Chem.*, 2005, **3**, 1013.
- 35 D. Parker, P. K. Senanayake and J. A. G. Williams, *J. Chem. Soc., Perkin Trans. 2*, 1998, 2129.
- 36 C. S. Bonnet and T. Gunnlaugsson, *New J. Chem.*, 2009, **33**, 1025.
- 37 C. Wei, H. Wei, W. Yan, Z. Zhao, Z. Cai, B. Sun, Z. Meng, Z. Liu, Z. Bian and C. Huang, *Inorg. Chem.*, 2016, **55**, 10645.





- 38 A. P. de Silva, H. Q. N. Gunaratne and T. E. Rice, *Angew. Chem., Int. Ed.*, 1996, **35**, 2116.
- 39 B. Song, G. Wang, M. Tan and J. Yuan, *J. Am. Chem. Soc.*, 2006, **128**, 13442.
- 40 M. Chen, Y. Zheng, J. Gao and Q. Wang, *Opt. Mater.*, 2016, **60**, 1.
- 41 M. P. Lowe, D. Parker, O. Reany, S. Aime, M. Botta, G. Castellano, E. Gianolio and R. Pagliarin, *J. Am. Chem. Soc.*, 2001, **123**, 7601.
- 42 R. S. Dickins, S. Aime, A. S. Batsanov, A. Beeby, M. Botta, J. I. Bruce, J. A. K. Howard, C. S. Love, D. Parker, R. D. Peacock and H. Puschmann, *J. Am. Chem. Soc.*, 2002, **124**, 12697.
- 43 K. Hanaoka, K. Kikuchi, H. Kojima, Y. Urano and T. Nagano, *J. Am. Chem. Soc.*, 2004, **126**, 12470.
- 44 O. Kotova, S. Comgy and T. Gunnlaugsson, *Chem. Commun.*, 2011, **47**, 6810.
- 45 A. M. Nonat, A. J. Harte, K. Sénéchal-David, J. P. Leonard and T. Gunnlaugsson, *Dalton Trans.*, 2009, 4703.
- 46 G. A. Crosby, R. E. Whan and R. M. Alire, *J. Chem. Phys.*, 1961, **34**, 743.
- 47 S. Tobita, M. Arakawa and I. Tnaka, *J. Phys. Chem.*, 1984, **88**, 2697.
- 48 S. Tobiata, *J. Phys. Chem.*, 1985, **89**, 5649.
- 49 F. Mian, G. Bottaro, R. Seraglia, M. Cavazzini, S. Quici and L. Armelao, *ChemPhysChem*, 2016, **17**, 3229.
- 50 G. Bottaro, F. Rizzo, M. Cavazzini, L. Armelao and S. Quici, *Chem. – Eur. J.*, 2014, **20**, 4598.
- 51 S. Quici, G. Marzanni, A. Forni, G. Accrosi and F. Barigelletti, *Inorg. Chem.*, 2004, **43**, 1294.
- 52 S. Quici, G. Marzanni, M. Cavazzini, P. L. Anelli, M. Botta, E. Gianolio, G. Accorsi, N. Armaroli and F. Barigelletti, *Inorg. Chem.*, 2002, **41**, 2777.
- 53 S. Quici, M. Cavazzini, M. C. Raffo, M. Botta, G. B. Giovenzana, B. Ventura, G. Accorsi and F. Barigelletti, *Inorg. Chim. Acta*, 2007, **360**, 2549.
- 54 S. Quici, M. Cavazzini, G. Marzanni, G. Accorsi, N. Armaroli, B. Ventura and F. Barigelletti, *Inorg. Chem.*, 2005, **44**, 529.
- 55 L. J. Daumann, D. S. Tatum, C. M. Andolina, J. I. Pacold, A. D'Aléo, G.-L. Law, J. Xu and K. N. Raymond, *Inorg. Chem.*, 2016, **55**, 114.
- 56 A. de Bettencourt-Dias, P. S. Barber and S. Bauer, *J. Am. Chem. Soc.*, 2012, **134**, 6987.
- 57 S. Petoud, S. M. Cohen, J.-C. G. Bünzli and K. N. Raymond, *J. Am. Chem. Soc.*, 2003, **125**, 13324.
- 58 B.-L. An, X.-D. Huang, J.-M. Zhang, X.-Y. Zhu and J.-Q. Xu, *J. Lumin.*, 2017, **187**, 340.
- 59 M. Xiao and P. R. Selvin, *J. Am. Chem. Soc.*, 2001, **123**, 7067.
- 60 M. Sy, D. Esteban-Gómez, C. Platas-Iglesias, A. Rodríguez-Rodríguez, R. Tripiet and L. J. Charbonnière, *Chem. – Eur. J.*, 2017, **14**, 2122.
- 61 A. Beeby, L. M. Bushby, D. Maffeo and J. A. G. Williams, *J. Chem. Soc., Dalton Trans.*, 2002, 48.
- 62 L. R. Melby, N. J. Rose, E. Abramson and J. C. Caris, *J. Am. Chem. Soc.*, 1964, **86**, 5117.
- 63 V.-M. Mikkala, H. Takalo, P. Liitti and I. Hemmilä, *J. Alloys Compd.*, 1995, **225**, 507.
- 64 V.-M. Mikkala, C. Sund, M. Kwiatkowski, P. Pasanen, M. Högberg, J. Kankare and H. Takalo, *Helv. Chim. Acta*, 1992, **75**, 1621.
- 65 V.-M. Mikkala, H. Helenius, I. Hemmilä, J. Kankare and H. Takalo, *Helv. Chim. Acta*, 1993, **76**, 1361.
- 66 X. Liu, Z. Tang, B. Song, H. Ma and J. Yuan, *J. Mater. Chem. B*, 2017, **5**, 2849.
- 67 Z. Dai, L. Tian, B. Song, Z. Ye, X. Liu and J. Yuan, *Anal. Chem.*, 2014, **86**, 11883.
- 68 M. Liu, Z. Ye, C. Xin and J. Yuan, *Anal. Chim. Acta*, 2013, **761**, 149.
- 69 Z. Dai, L. Tian, Z. Ye, B. Song, R. Zhang and J. Yuan, *Anal. Chem.*, 2013, **85**, 11658.
- 70 Y. Xiao, R. Zhang, Z. Ye, Z. Dai, H. An and J. Yuan, *Anal. Chem.*, 2012, **84**, 10785.
- 71 Y. Xiao, Z. Ye, G. Wang and J. Yuan, *Inorg. Chem.*, 2012, **51**, 2940.
- 72 C. Piguet and J.-C. G. Bünzli, *Handbook on The Physics and Chemistry of Rare Earths*, Elsevier, 2010, pp. 301–553.
- 73 M. Hasegawa, H. Ohtsu, D. Kodama, T. Kasai, S. Sakurai, A. Ishii and K. Suzuki, *New J. Chem.*, 2014, **38**, 1225.
- 74 H. Wada, S. Ooka, D. Iwasawa, M. Hasegawa and T. Kajiwara, *Magnetochemistry*, 2016, **2**, 43.
- 75 N. Goto, A. Ishii, S. Ogata, K. Kondo, K. Yoshihara, J. Tsuchiyagaito, S. Kawaguchi, K. Sugimoto and M. Hasegawa, in preparation to submit to RSC soon.
- 76 K. E. Andersen, J. L. Sørensen, P. O. Huusfeldt, L. J. S. Knutsen, J. Lau, B. F. Lundt, H. Petersen, P. D. Suzdak and M. D. B. Swedberg, *J. Med. Chem.*, 1999, **42**, 4281.
- 77 G. H. Dieke and H. M. Crosswhite, *Appl. Opt.*, 1963, **2**, 675.
- 78 S. Comby, D. Imbert, A.-S. Chauvin and J.-C. G. Bünzli, *Inorg. Chem.*, 2006, **45**, 732.
- 79 C. Y. Chow, S. V. Eliseeva, E. R. Trivedi, T. N. Nguyen, J. W. Kampf, S. Petoud and V. L. Pecorato, *J. Am. Chem. Soc.*, 2016, **138**, 5100.
- 80 S. Ogata, A. Ishii, C. L. Lu, T. Kondo, N. Yajima and M. Hasegawa, *J. Photochem. Photobiol., A*, 2017, **334**, 55.
- 81 M. Latva, H. Takalo, V.-M. Mikkala, C. Matachescu, J. C. Rodríguez-Ubis and J. Kankare, *J. Lumin.*, 1997, **75**, 149.
- 82 S. Katagiri, Y. Hasegawa, Y. Wada and S. Yanagida, *Chem. Lett.*, 2004, **33**, 1438.
- 83 W. T. Carnall, P. R. Fields and K. Rajnak, *J. Chem. Phys.*, 1968, **49**, 4447.
- 84 J. L. Kropp and M. W. Windsor, *J. Chem. Phys.*, 1963, **39**, 2769.
- 85 J. L. Kropp and M. W. Windsor, *J. Chem. Phys.*, 1965, **42**, 1599.
- 86 J. L. Kropp and M. W. Windsor, *J. Chem. Phys.*, 1966, **45**, 761.
- 87 A. Heller, *J. Am. Chem. Soc.*, 1966, **88**, 2058.



- 88 J. L. Kropp and M. W. Windsor, *J. Phys. Chem.*, 1967, **71**, 477.
- 89 Y. Hass and G. Stein, *J. Phys. Chem.*, 1972, **76**, 1093.
- 90 G. Stein and E. Wurzburg, *J. Chem. Phys.*, 1975, **62**, 208.
- 91 Y. Hass and G. Stein, *J. Phys. Chem.*, 1971, **75**, 3668.
- 92 Y. Hass and G. Stein, *J. Phys. Chem.*, 1971, **75**, 3677.
- 93 W. D. Horrocks, Jr. and D. R. Sudnick, *J. Am. Chem. Soc.*, 1979, **101**, 334.
- 94 W. D. Horrocks, Jr. and D. R. Sudnick, *Acc. Chem. Res.*, 1981, **14**, 384.
- 95 R. M. Supkowski and W. D. Horrocks, Jr., *Inorg. Chim. Acta*, 2002, **340**, 44.
- 96 H. Ohashi, K. Tanigaki, R. Kumashiro, S. Sugihara, S. Hiroshiba, S. Kimura, K. Kato and M. Takata, *Appl. Phys. Lett.*, 2004, **84**, 520.

